Mossbauer spectra of antiferromagnetic powders in applied fields

1990 J. Phys.: Condens. Matter 2 7329

(http://iopscience.iop.org/0953-8984/2/35/008)

J. Phys.: Condens. Matter 2 (1990) 7329–7337. Printed in the UK

Mössbauer spectra of antiferromagnetic powders in applied fields

Q A Pankhurst† and R J Pollard‡

† Department of Physics, University of Liverpool, Liverpool L69 3BX, UK

‡ Department of Physics, Monash University, Clayton, Victoria 3168, Australia

Received 30 January 1990, in final form 24 April 1990

Abstract. The problem of interpreting Mössbauer spectra of antiferromagnetic powders subject to applied magnetic fields is considered. A mean-field model for systems with uniaxial anisotropy is used to fit simultaneously spectra taken with applied fields of different strengths. The model predicts a variety of asymmetric broad line profiles depending on the strengths of the exchange and anisotropy terms. The method is applied to the 4.2 K spectra of goethite and haematite subject to longitudinal applied fields of 0, 3, 6 and 9 T. Favourable agreement is obtained with the results from single crystals, showing that the method can be reliably used for a variety of antiferromagnetic materials.

1. Introduction

An understanding of the nature of the atomic exchange and anisotropy interactions in magnetic materials is often of great importance, both for unravelling the physics of the materials and for furthering the success of any technological applications. For example the exchange constant J is closely related to the magnetic ordering temperature, and the anisotropy constant K is the origin of such macroscopic parameters as the magnetic coercivity and the superparamagnetic 'blocking' temperature.

One method of deducing J and K is to apply an external magnetic field to the sample and measure the resultant equilibrium orientations of the atomic moments, via neutron diffraction or Mössbauer spectroscopy, for example. This method is particularly direct in the case of antiferromagnetic single-crystal samples for which, if the applied field is perfectly aligned with the easy anisotropy axis, a first-order 'spin-flop' phase transition occurs at a critical field $B_{sf} \simeq \sqrt{2B_E B_A}$, where B_E and B_A are the effective fields corresponding to J and K respectively. At the transition point the antiferromagnetic axis of the moments reorients or 'flops' to a direction perpendicular to the easy axis, and as such is simple to recognise experimentally. However, if the applied field is misaligned by an angle in excess of $\sim B_A/2B_E$ the transition is no longer sharp, and a gradual reorientation is observed [1,2]. The situation is further complicated in the case of polycrystalline samples for which the angle between the applied field and the easy axis is evenly distributed between 0 and π: the experimental signal is then a superposition of all the constituent crystallites' signals, and there is a resultant loss in the definition of the transition. Consequently it is evident in the literature that the spin-flop method of measuring B_E and B_A is generally only used for well characterised single crystal samples.

0953-8984/90/357329+09$03.50

However, there are numerous occasions when it is either necessary or desirable to work with powder samples. In many cases the sample is only available in polycrystalline form, as in, e.g., biomineral proteins such as ferritin and haemosiderin, or in geological specimens in soils, etc. The polycrystalline form itself may be relevant, for example in studies of particulate magnetic recording media and in some types of catalyst. The use of powder samples can often dramatically improve the experimental signal-to-noise ratio, reducing the recording time needed and improving the accuracy of measured parameters. Also, the random nature of the powder itself may simplify analysis, especially compared to poorly characterised single crystals for which mosaicity and uncertainties in alignment can be problematic.

Computer programs have been available for many years to analyse the Mössbauer spectra of powders in applied fields with certain assumptions. The PDRHXT program by Gabriel and Ruby [3] sums single-crystal spectra over a range of orientations of the electric field gradient (EFG) axes in order to represent random crystallite orientations, however it does not perform a summation of internal and external fields. A program by Lang and Dale [4] uses a spin Hamiltonian to calculate both the magnetic interaction between electron spins and the nucleus and the direct nuclear Zeeman interaction with the applied field. Here the internal field is assumed to be proportional to the applied field, and hence the program is appropriate for diamagnets and paramagnets. More recently Blaes *et al* have derived analytic expressions for the lineshapes in these cases [5].

Two different analyses of the spectra of antiferromagnetic goethite have been reported by De Grave and coworkers. In one, a single angle of 80° between the EFG principal axis and the hyperfine field was assumed [6]. In the other, a model-independent technique was used to obtain a two-dimensional probability distribution of both the hyperfine field and the orientation of the field with the external field [7]. In the model-independent technique interpretation of the distribution is difficult.

In this work we use a simple mean-field model to show that the Mössbauer spectra of antiferromagnetic powders in applied fields have lineshapes that in many cases depend critically on the exchange and anisotropy fields, offering a simple 'fingerprinting' technique for determining these parameters from powder data. As illustration we consider the spectra of polycrystalline goethite and haematite.

2. Method

The Hamiltonian for a uniaxial antiferromagnet subject to an external applied field B incorporates exchange, anisotropy and applied field terms:

$$H = -2J\sum_{ij} \boldsymbol{S}_i \cdot \boldsymbol{S}_j - K\left(\sum_i (S_{zi})^2 + \sum_j (S_{zj})^2\right) - g\mu_B \boldsymbol{B} \cdot \left(\sum_i \boldsymbol{S}_i + \sum_j \boldsymbol{S}_j\right). \quad (1)$$

Here $J < 0$ is the exchange constant, $K > 0$ is the anisotropy constant, g is the spectroscopic splitting factor, μ_B is the Bohr magneton, and $\boldsymbol{S}_i$ and $\boldsymbol{S}_j$ refer to spins on the two different sublattices. Using the mean field approximation the energy of the system can be expressed in terms of the orientations of the two sublattice spins:

$$E = NSg\mu_B\{B_E\cos(\theta_1 - \theta_2) - \tfrac{1}{2}B_A[\cos^2(\theta_1 - t) + \cos^2(\theta_2 - t)] - B(\cos\theta_1 + \cos\theta_2)\} \quad (2)$$

where θ_1, θ_2 and t are the polar angles of the sublattice spins (θ_1,θ_2) and the easy anisotropy axis (t) with respect to the applied field direction. The exchange field is defined as $B_E=-2JzS/g\mu_B$ where z is the number of exchange-coupled neighbours of a given spin, and the anisotropy field is given by $B_A=2KS/g\mu_B$. For a given t the equilibrium spin configuration is obtained by solving the simultaneous equations $\partial E/\partial\theta_1 = \partial E/\partial\theta_2 = 0$. In a powder the angle t is sampled continuously from 0 to π, although for an antiferromagnet the range 0 to $\pi/2$ encompasses all unique solutions.

The Mössbauer spectrum of a polycrystalline absorber is therefore a $(\sin t)$-weighted superposition of the subspectra corresponding to each individual value of t. It may be modelled by choosing a finite number (N_t) of representative values of t (e.g. $t = \cos^{-1}[(2n-1)/2N_t]$, $n = 1, \ldots, N_t$), solving equation (2) for the equilibrium spin directions, and calculating and summing the resulting subspectra. The choice of N_t is largely determined by the available computer resources—in practice we have found $N_t \sim 20$ to be a suitable approximation.

Simulated ^{57}Fe Mössbauer spectra, obtained using the above method, are shown in figures 1 and 2. Parameters of relevance to high-spin Fe^{3+} compounds were used: linewidth $\Gamma = 0.26$ mm s^{-1}, hyperfine field $B_{hf} = 50$ T, exchange field $B_E = 300$ T, and anisotropy fields $B_A = 0$, 0.03, 0.10, 0.25, 0.50 and 300 T. For clarity the isomer shift δ and the quadrupole splitting Δ were both taken to be zero. For each value of B_A four spectra are simulated, for applied fields $B = 0$, 3, 6 and 9 T. The two most common experimental geometries are shown: 'longitudinal drive', in which the γ-ray beam is directed parallel to $\boldsymbol{B}$ (figure 1), and 'transverse drive', in which the γ-rays are perpendicular to $\boldsymbol{B}$ (figure 2).

The lineshapes of the simulated spectra may be understood by recalling that in a magnetically split ^{57}Fe spectrum with negligible electric quadrupole interaction the relative intensities of the outer : middle : inner pairs of lines are given by the radiation probabilities

$$3(1+\cos^2\theta) : 4\sin^2\theta : (1+\cos^2\theta) \tag{3}$$

where θ is the angle between the incident γ-ray and the effective field $\boldsymbol{B}_{eff}$. Here $\boldsymbol{B}_{eff}$ is obtained by the vector addition of $\boldsymbol{B}$ and $\boldsymbol{B}_{hf}$, where the orientation of $\boldsymbol{B}_{hf}$ has been determined by solving equation (2) and the magnitude of B_{hf} is assumed to be single valued.

In zero applied field $\boldsymbol{B}_{eff} \equiv \boldsymbol{B}_{hf}$ and there is an isotropic distribution of θ over a sphere, giving $\overline{\sin^2\theta} = \frac{2}{3}$ and relative line intensities $\frac{12}{3} : \frac{8}{3} : \frac{4}{3}$, i.e. 3 : 2 : 1. In the limit of zero anisotropy ($B_A = 0$) the spins are completely free to reorient in response to a non-zero applied field and 'flop' to a direction perpendicular to $\boldsymbol{B}$. In longitudinal drive this gives $\theta = 90°$ for all the spins and 3 : 4 : 1 spectra; in transverse drive the γ-rays encounter a disc of spins giving $\overline{\sin^2\theta} = \frac{1}{2}$ and intensities $\frac{9}{2} : \frac{4}{2} : \frac{3}{2}$, i.e. 3 : $\frac{4}{3}$: 1.

In the limit of very large anisotropy (represented by $B_A = 300$ T) the spins are essentially fixed in space, irrespective of the applied field. The effective fields are therefore the vector sums of $\boldsymbol{B}$ and an isotropic spherical distribution of the $\boldsymbol{B}_{hf}$. Thus the majority of the $\boldsymbol{B}_{eff}$ are approximately perpendicular to $\boldsymbol{B}$, with magnitudes $\overline{B_{eff}} \sim \sqrt{B_{hf}^2 + B^2}$; relatively few are approximately parallel to $\boldsymbol{B}$, with magnitudes $B_{eff}^{max} \sim B_{hf} + B$; even fewer are approximately antiparallel to $\boldsymbol{B}$, with magnitudes $B_{eff}^{min} \sim B_{hf} - B$. In longitudinal drive the B_{eff}^{max} and B_{eff}^{min} contributions have $\overline{\sin^2\theta} \simeq 0$ and intensities of order 6 : 0 : 2, so that they dominate the lineshapes of the outermost lines. In transverse drive the $\overline{B_{eff}}$ sites have approximately $\frac{9}{2} : 2 : \frac{3}{2}$ subspectra while

Figure 1. Simulated ^{57}Fe Mössbauer spectra of a powdered uniaxial antiferromagnet with hyperfine field B_{hf} = 50 T and exchange field B_E = 300 T subject to longitudinal magnetic fields of strength B = 0, 3, 6 and 9 T. Sets of spectra are shown for anisotropy fields B_A = 0, 0.03, 0.10, 0.25, 0.50 and 300 T.

the B_{eff}^{max} and B_{eff}^{min} sites make 3 : 4 : 1 contributions which are most readily apparent in the shapes of the second and fifth lines of the sextet.

At intermediate anisotropies one of the most noticeable features is that the spin-flop transition may be discerned for those crystallites where the easy anisotropy axis is close to $\boldsymbol{B}$. For B_A = 0.03 T the critical field $B_{sf} \simeq 4.2$ T; consequently in the

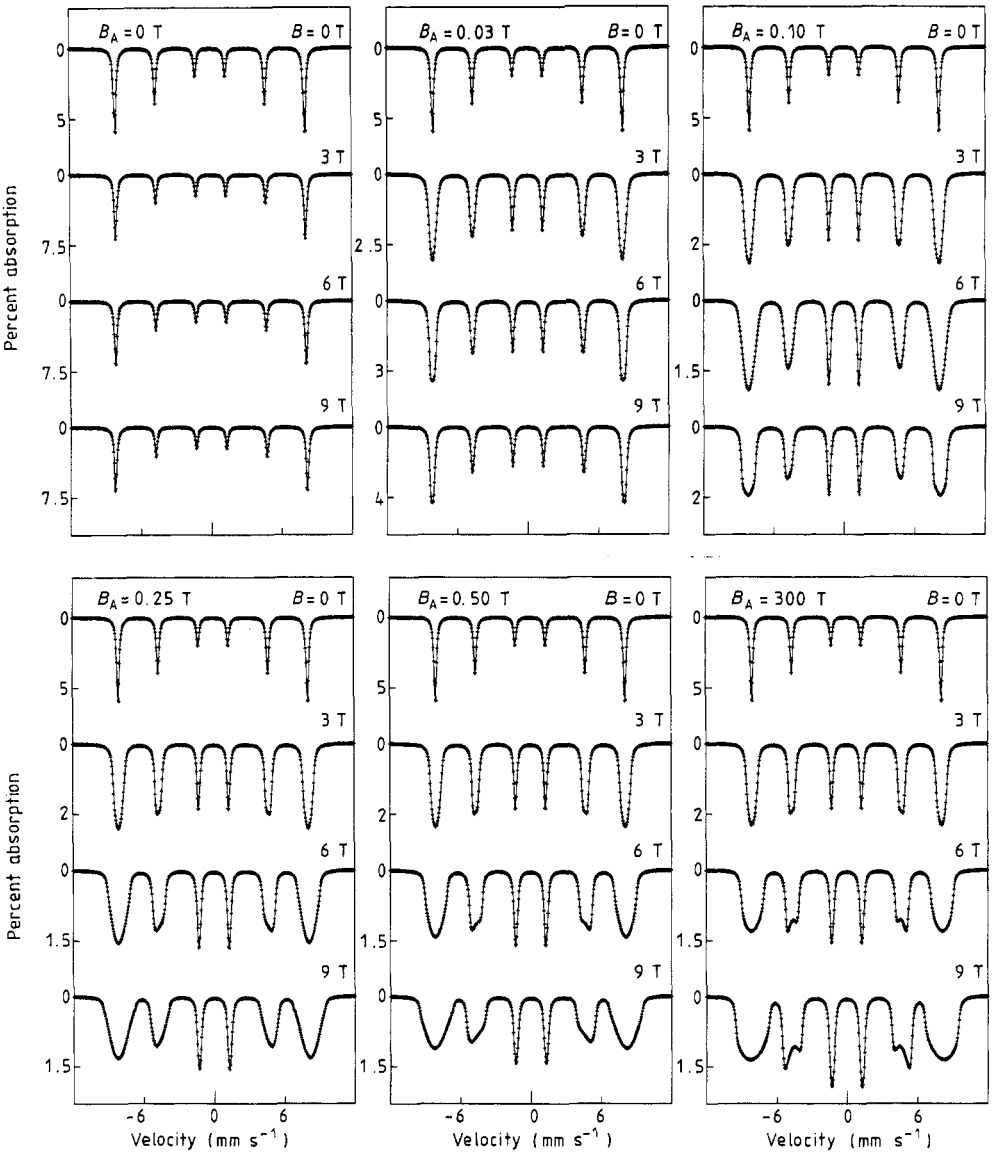

Figure 2. Simulated Mössbauer spectra corresponding to those of figure 1, but with a transverse drive geometry.

$B = 3$ T spectrum the outer lines are broadened by $\Delta B_{\text{eff}} = B_{\text{eff}}^{\text{max}} - B_{\text{eff}}^{\text{min}} \simeq 6$ T while in the $B = 6$ T and 9 T spectra these spins have reoriented to be perpendicular to $\boldsymbol{B}$ and the lines are relatively narrow. For $B_A = 0.10$ T $B_{\text{sf}} \simeq 7.7$ T and the $B = 3$ T and 6 T spectra are broadened by $\Delta B_{\text{eff}} \simeq 6$ T and 12 T respectively while the $B = 9$ T spectrum is relatively narrow, with $\Delta B_{\text{eff}} \ll 18$ T. For $B_A = 0.25$ T and 0.50 T $B_{\text{sf}} > 9$ T and all the spectra are broad. These effects are most easily seen in the longitudinal drive geometry.

In the simulations of figures 1 and 2 the quadrupole splitting Δ was taken to be zero. However, in reality Δ is usually of order 0.6 mm s^{-1} in ferric compounds, and is apparent in each subspectrum as a 'quadrupole shift' of the centroid of the inner four lines relative to the centroid of the outer two lines. In the simple case of an axially symmetric electric field gradient (EFG) this shift is $2\epsilon = \frac{1}{2}(3\cos^2\xi - 1)\Delta$, where ξ is the angle between $\boldsymbol{B}_{\text{eff}}$ and the EFG principal axis. The way in which this affects the applied field spectra depends on the relative orientations of the EFG principal axis and the easy anisotropy axis (see section 4).

A second assumption used in the above simulations that may not always be valid is that B_{hf} is independent of B. In low dimensional magnets there is sometimes a pronounced minimum in B_{hf} at the spin-flop field, resulting from the applied field dependence of spin-wave fluctuations [8]. Such effects are sometimes present, though reduced, in three-dimensional magnets. Another effect occurs if B_{hf} is not saturated, i.e. if the experimental sample temperature is not well below the Néel temperature T_N. In this case the critical point of the field-induced phase transition between antiferromagnetic and paramagnetic phases may be lowered considerably, leading to a strongly B-dependent hyperfine field [9].

Also, an isotropic distribution of the crystallites' orientations over a sphere may not always be realised. Powder absorbers sometimes exhibit texture resulting from an intrinsic preferred orientation of the crystallites; this is evidenced by a departure from the intensity ratio 3:2:1 in the zero applied field spectra. The subspectral weighting function $f(t)$ in these cases will not be $\sin t$, but some other function that may either be modelled or experimentally determined as a probability distribution by appropriately fitting the $B = 0$ spectra.

In concluding this section we note that although the discussion above has referred to ferric iron only, the method is equally applicable to ferrous iron as well as many other Mössbauer isotopes.

3. Experimental details

Samples of goethite and haematite particles were selected for Mössbauer experiments; at 4.2 K both materials are antiferromagnets. Transmission electron microscopy showed that the haematite sample (Johnson–Matthey, purity > 99.999%) consisted of spheroidal particles of diameter 0.5–1.0 μm. Goethite was obtained from the precipitate of a ferric nitrate solution induced by adding potassium hydroxide. These particles were rod-shaped with width 14 ± 4 nm and length 70 ± 10 nm. No impurities were present in x-ray diffractograms of either sample.

Mössbauer absorbers were prepared by mixing the powders with boron nitride and clamping between plastic discs. Thicknesses were of order 11 mg cm^{-2} of the compound. A ^{57}Co:Rh source at 4.2 K was used, and velocity calibration was with respect to the centre of a spectrum of iron foil at room temperature. The velocity waveform was triangular shaped; spectra with 500 channels were obtained after numerical folding to remove baseline curvature.

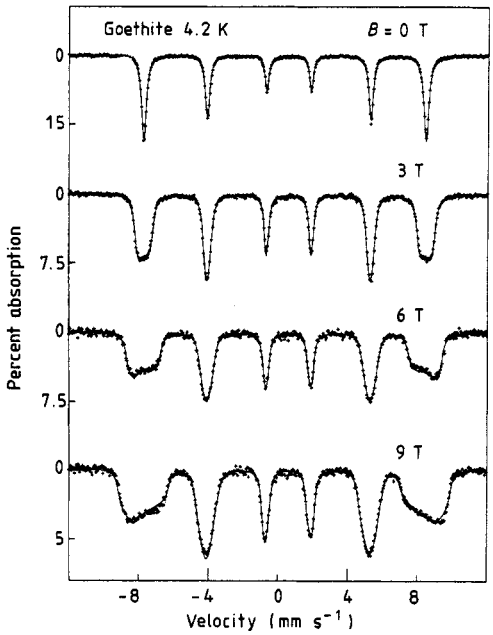

Figure 3. Spectra of goethite at 4.2 K, longitudinal drive geometry. The solid lines were obtained by simultaneously fitting all four spectra using the model described in the text.

4. Experimental results

4.1. Goethite

Spectra of a polycrystalline sample of goethite, α-FeOOH, recorded at 4.2 K in longitudinal drive geometry, are shown in figure 3.

All four spectra in the figure were least-squares fitted simultaneously. As a first-order approximation the EFG was taken to be axially symmetric, even though the detailed description of the EFG asymmetry is known to be somewhat complicated [10]. The EFG principal axis was taken to be perpendicular to the easy anisotropy axis. The linewidths of the outer and inner pairs of lines were allowed to be incrementally broader and narrower than the middle pairs of lines as a means of taking into account a small degree of sample inhomogeneity. The hyperfine field was taken to be independent of the applied field. Lastly, the exchange field was constrained to the value $B_E = 290$ T, in keeping with a recent measurement of the exchange constant in goethite of $J/k_B \simeq 13$ K [11].

The following parameters were obtained: $\delta = 0.49$ mm s^{-1}, $\Delta = 0.49$ mm s^{-1}, $\Gamma = 0.27$ mm s^{-1}, $\Delta\Gamma = 0.04$ mm s^{-1}, $B_{hf} = 50.1$ T and $B_A = 0.41$ T. The low values of Γ and $\Delta\Gamma$ indicate that the model has accounted for nearly all of the line broadening. The uncertainty in B_A was estimated by monitoring the goodness-of-fit parameter, χ^2; similar quality fits lay in the range 0.34–0.54 T.

As a result of the simultaneous fitting procedure the problems associated with the

interdependence of the fit parameters were largely eliminated. Since B_E and B_A have no effect on the zero applied field spectrum, a good fit of that spectrum determines the parameters $\delta, \Delta, \Gamma, \Delta\Gamma$ and B_{hf}; subsequently the fit of the non-zero applied field spectra determines B_E and B_A. The interdependence of B_E and B_A was avoided by constraining B_E to the known value, leaving B_A as the only free parameter.

The overall quality of the fit is good, implying that the uniaxial anisotropy approximation, although not strictly valid [12], is quite adequate for describing the applied field response of goethite. Using the fitted parameters a spin-flop critical field of $B_{sf} \simeq 15.4$ T is predicted. This is consistent with a previous search for a spin-flop in single crystal goethite which yielded $B_{sf} > 10.0$ T [12]. The result that $B_A \simeq 0.41$ T represents the first time that the anisotropy field in goethite has been determined, as opposed to a lower limit having been set.

4.2. Haematite

The spectra of powdered haematite, α-Fe_2O_3, recorded at 4.2 K in longitudinal drive geometry, are shown in figure 4.

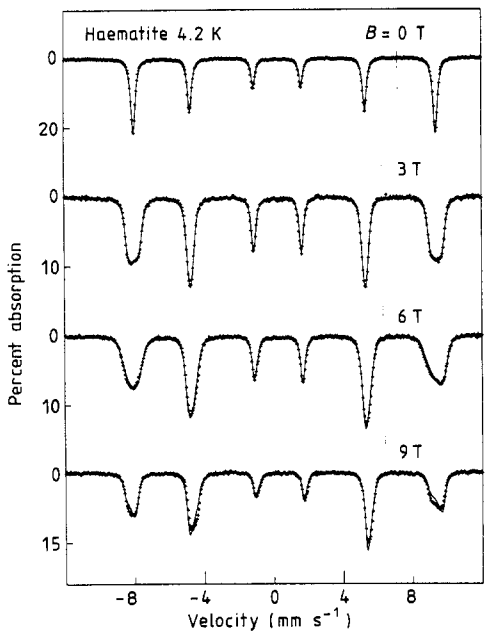

Figure 4. Spectra of haematite at 4.2 K, longitudinal drive geometry. The solid lines were obtained by simultaneously fitting all four spectra.

The calculated spectra incorporated the following constraints: the EFG in haematite is symmetric, and the principal axis is parallel to the easy axis; to first-order B_{hf} was taken to be independent of B, ignoring the ~1.5% decrease observed at the spin-flop transition in single crystals [13]; and the exchange field was fixed at $B_E = 972$ T [14].

The parameters from the fit were: $\delta = 0.49$ mm s^{-1}, $\Delta = 0.40$ mm s^{-1}, $\Gamma = 0.27$ mm s^{-1}, $\Delta\Gamma = 0.02$ mm s^{-1}, $B_{hf} = 53.8$ T and $B_A = 0.02$ T. Upper and lower

limits for B_A were estimated as 0.022 T and 0.019 T respectively. The predicted spin-flop field is ~ 6.2 T, which compares favourably with the $B_{sf} \simeq 6.4$ T value measured in single crystals [13].

The quality of the fit is reasonable for the $B = 0$, 3 and 6 T spectra, but rather poor for the $B = 9$ T spectrum. Since only in the 9 T spectrum is $B > B_{sf}$ it is reasonable to attribute this poor fit to a breakdown in the uniaxial anisotropy approximation with relation to the spin-flop phase. To model haematite more accurately it may be necessary to include the Dzyaloshinskii anisotropy term in the mean field Hamiltonian, equation (1), and proceed accordingly.

5. Conclusions

The application of applied field Mössbauer spectroscopy to the determination of the exchange and anisotropy characteristics of antiferromagnetic powders gives reliable results while retaining the advantages of working with powder samples: availability, high counting rate, improved signal-to-noise ratio, etc. Although in this paper we have presented the method with reference to the simple model of uniaxial anisotropy, in principle the method may be easily extended to more complex forms of anisotropy. However, there may be a limit to the complexity of model that can be conveniently dealt with—largely determined by the speed of computation available to the user. Also, in the case of poorly characterised materials, e.g. those with a large internal distribution of hyperfine fields, the spectral interpretation may be significantly less straightforward. However, it is clear that the method has great potential for future application; in our laboratories work is currently in progress to investigate such diverse magnetic materials as barium ferrite, ferrihydrite and human ferritin.

Acknowledgments

We are grateful to D G Lewis (Waite Agricultural Research Institute) for preparing the goethite sample, and to the Australian Research Council for financial support.

References

[1] Jones D H and Pankhurst Q A 1987 *J. Phys. C: Solid State Phys.* **20** 2453–63
[2] Pankhurst Q A, Johnson C E, Jones D H and Thomas M F 1988 *Hyperfine Interact.* **41** 505–8
[3] Gabriel J R and Ruby S L 1965 *Nucl. Instrum. Methods* **36** 23–8
[4] Lang G and Dale B W 1974 *Nucl. Instrum. Methods* **116** 567–71
[5] Blaes N, Fischer H and Gonser U 1985 *Nucl. Instrum. Methods Phys. Res.* B **9** 201–8
[6] De Grave E and Vandenberghe R E 1986 *Hyperfine Interact.* **28** 643–6
[7] Bowen L H, De Grave E, de Bakker P M A and Vandenberghe R E 1990 *Proc. Int. Conf. on the Applications of the Mössbauer Effect, Budapest, 1989, Hyperfine Interact.* **53–57**
[8] Jones D H, Pankhurst Q A and Johnson C E 1987 *J. Phys. C: Solid State Phys.* **20** 5149–59
[9] Boersma F, Cooper D M, de Jonge W J M, Dickson D P E, Johnson C E and Tinus A M C 1982 *J. Phys. C: Solid State Phys.* **15** 4141–5
[10] Meagher A and Pankhurst Q A 1987 *Phys. Status Solidi* **101** K73–6
[11] De Grave E 1990 *Proc. 24th Zakopane School on Physics* vol 2 (Singapore: World Scientific)
[12] Meagher A, Pankhurst Q A and Dickson D P E 1986 *Hyperfine Interact.* **28** 533–6
[13] Pankhurst Q A, Johnson C E and Thomas M F 1986 *J. Phys. C: Solid State Phys.* **19** 7081–98
[14] Jacobs I S, Beyerlein R A, Foner S and Remeika J P 1971 *Int. J. Magn.* **1** 193